Journal of Applied Polymer Science

Preparation of water-compatible antifungal polyurethane with grafted benzimidazole as the antifungal agent

Yong-Chan Chung,[1] Ha Youn Kim,[2] Jae Won Choi,[2] Byoung Chul Chun[2]
[1]Department of Chemistry, University of Suwon, Hwaseong 445-743, Korea
[2]School of Nano Engineering, Inje University, Gimhae 621-749, Korea
Correspondence to: B. C. Chun (E-mail: bcchun@inje.ac.kr)

ABSTRACT: We compared two series of benzimidazole (BI)-grafted polyurethane (PU), one of which was water-compatible, to compare their antifungal activities. The water-compatible PU series had an additional 2,2-bis(hydroxymethyl)propanoic acid group in the PU backbone. The water-compatible PU series had a lower crosslinking density and tensile strength compared to the other PU series with increasing BI content. Although ordinary PU did not suppress fungal growth (*Chaetomium globosum*), the water-compatible PU completely suppressed the growth even though it contained half as many BI groups. © 2014 Wiley Periodicals, Inc. J. Appl. Polym. Sci. **2015**, *132*, 41676.

KEYWORDS: elastomers; functionalization of polymers; grafting; polyurethanes

Received 13 June 2014; accepted 20 October 2014
DOI: 10.1002/app.41676

INTRODUCTION

Antimicrobial polymeric materials have been extensively researched and used in automotive interiors, fibers, healthcare products, coatings, packaging, and household appliances.[1] Antimicrobial activity is conferred to the polymer by grafting or the addition of antimicrobial agents; these include phosphonate groups, sulfonate groups,[2] quaternary ammonium groups,[3] zinc oxide,[4] nanoparticles,[5] or silver ions.[6–8] Benzimidazole (BI) derivatives are well-known heterocyclic bioactive compounds that exhibit broad-spectrum antifungal and antibacterial activities, and several BI derivatives have been synthesized and tested for antimicrobial activity.[9–12] Antifungal agents are mainly classified into polyenes, azoles, allylamines, and echinocandins, in which the azole class antifungal agents have been the most widely studied and used. Amphotericin B, a polyene class antifungal agent, has been used for more than 40 years, but a significant nephrotoxicity was found for this agent. However, imidazole and triazole antifungal agents introduced in early 1990s have safely treated fungal infections, and their safety records have led to their extensive use. Azole class antifungal medications including BI are known to block the function of lanosterol 14-α-demethylase, a cytochrome P450 enzyme, which is necessary for converting lanosterol to ergosterol, which is an essential component of the fungal membrane. The egrosterol-deficient fungal membrane, having lost the flexibility of normal membrane, cannot control the permeation of ions and organic molecules through the membrane, and this eventually inhibits fungal growth.[13] Alternatively, BI can also be used in other applications. For example, the BI moiety has been used to prepare organic photovoltaic solar cell membranes to broaden their absorption wavelength range.[14,15] Poly(benzimidazole) membranes have been used as polymer electrolytes in fuel cell membranes because of their good fuel cell performance and durability.[16–18] A polyimide with a BI moiety was used to develop heat-resistant materials for electronics, coatings, and membranes.[19] A polymer-supported BI metal complex was used as a polymeric catalyst for oxidation reactions.[20] Polyurethane (PU) has been widely used for polymer backbones because of its exceptional properties, such as its excellent tensile properties and easy modification and functionalization and because of the high demand for it in coatings and textiles.[21–23] We demonstrated that the grafting of functional groups onto PU produces functionalized PUs from unfunctionalized PUs. For example, PUs that exhibited flexibility at low temperatures,[24] electric attraction in aqueous solutions,[25] magnetism,[26] pH-indicating abilitiy,[27] and photoluminescence[28] have been developed. However, the development of antifungal PUs with antifungal agents has not been reported so far, although some antimicrobial polymers containing quaternary ammonium groups have been researched.[29,30] Therefore, it should be straightforward to graft BI onto PU to provide it with antifungal activity because of the effective inhibitory activity of BI against various microorganisms. Antifungal PUs may have broad applications in such areas as automobile seat foams, thermal insulation foams, elastic textiles, protective wood coatings, book binding glues, and

Table I. PU Compositions

Sample code[a]	Reactant (mmol)						
	MDI-1	PTMG	MDI-2	BD	DMPA[a]	MDI-3[b]	BI
B-1	20	20	30	30	—	—	—
B-2	20	20	30	30	—	1	1
B-3	20	20	30	30	—	2	2
B-4	20	20	30	30	—	3	3
B-5	20	20	30	30	—	4	4
DB-1	20	20	30	25	5	1	2
DB-2	20	20	30	20	10	1	2
DB-3	20	20	30	15	15	1	2
DB-4	20	20	30	10	20	1	2
DB-5	20	20	30	5	25	1	2

[a] DMPA was used to improve the water compatibility.
[b] MDI-3 was used to graft BI onto the PU.

watch-band wrapping. In this study, BI was grafted onto PU, instead of blended with it, to strongly bind it to PU and ensure its homogeneous distribution throughout the PU. The water compatibility of the BI-grafted PU was improved through the introduction of carboxyl groups into the PU, and the properties of the BI-grafted PUs with and without carboxyl groups were compared. In this study, we investigated the following: the covalent grafting of BI onto PU, the effect of the PU water compatibility on its thermal and physical properties (tensile strength and shape recovery), and the antifungal activity of the PUs as a function of the BI content and water compatibility.

EXPERIMENTAL

Materials

Poly(tetramethylene glycol) (PTMG; number-average molecular weight = 2000 g/mol, Sigma-Aldrich, St. Louis, MO), 4,4′-methylenebis(phenyl isocyanate) (MDI; Junsei Chemical, Tokyo, Japan), and 1,4-butanediol (BD; Junsei Chemical) were dried overnight under high vacuum (0.1 Torr). BI and 2,2-bis(hydroxymethyl)propanoic acid (DMPA) were obtained from Sigma-Aldrich and were also vacuum-dried. Dimethylformamide (DMF; Duksan Chemical, Ansan, Korea) was distilled over CaH_2 before use.

Polymer Synthesis

MDI (MDI-1, 5.00 g, 20.0 mmol) was added to PTMG (40.0 g, 20.0 mmol) in a 500-mL, four-necked, beaker-type flask equipped with a mechanical stirrer, condenser, temperature-controlled heating mantle, and nitrogen purge. The mixture was allowed to react for 2 h at 50°C to produce the prepolymer. BD and DMPA were dissolved in 10 mL of DMF in the amounts specified in Table I and added to the prepolymer. The mixture was allowed to react for 1 h. Then, MDI (MDI-2, 7.50 g, 30.0 mmol) was added to the reaction mixture, and the reaction was continued for 1 h, during which 10 mL of DMF was slowly added via a dropping funnel to prevent a sudden increase in the viscosity. MDI (MDI-3) was subsequently added to the reaction mixture, and the reaction was continued for 40 min. Next, BI dissolved in 10 mL of DMF was added to the reaction mixture, and the reaction was continued for 2 h. Then, the product was precipitated in distilled water (1.5 L) to terminate the polymerization. The product was cut into pieces and thoroughly washed with distilled water (1.5 L × 3) and ethanol (1 L × 2) under magnetic stirring to remove any remaining reactants. The final product was suction-filtered and dried in an oven (60°C) for 3 days. The PU structure, grafting steps, and crosslinking structure are shown in Scheme 1. The mechanical and shape-memory test samples were prepared by solvent casting. Specifically, a PU solution in DMF was slowly evaporated at 60°C for 60 h to obtain a sheet (0.5 mm thick). The film thickness was measured with a digital caliper (Mitutoyo CD-15CPX, Tokyo, Japan), and the average thickness of five points was recorded. Specimens were prepared from the PU sheet according to ASTM D 638. Two sample series (DB and B series) were prepared: one series included the water compatibility agent, whereas the other did not.

Crosslinking Density

A 20 × 20 × 1 mm^3 specimen with a known weight (m_1) was swollen in 50 mL of toluene in a closed-cap bottle for 24 h. The swollen weight of the specimen (m_2) was measured after we quickly removed the adsorbed toluene from the polymer surface with a tissue. The swollen specimen was dried at room temperature for a week and then weighed to obtain the dry mass (m_3). The solvent volume in the swollen specimen (V_s) was calculated with the weight difference between the swollen (m_2) and dry states (m_3) and the solvent density (0.8699 g/cm^3) and averaged over five swelling experiments. We calculated the volume of the dried polymer (V_p) by dividing the polymer dry weight (m_1) by the polymer density. The volume fraction of the polymer in the swollen mass (v_1) was calculated as $V_p/(V_s + V_p)$. The derivation of the crosslinking density is described in the Results and Discussion section.

Spectroscopic, Viscosity, and Contact Angle Analysis

A Fourier transform infrared spectrophotometer (Jasco 300E, Tokyo, Japan) equipped for attenuated total reflectance measurements was used to collect the IR spectra. For each sample, 25 scans were performed with a resolution of 4 cm^{-1} and scan speed of 2 mm/s. The absorption spectra of the PU solutions (0.025 wt %) in DMF were collected over the range 300–700 nm with an ultraviolet–visible (UV–vis) spectrophotometer (Secomam Uvicon XS, France). The absolute viscosity of the samples dissolved in DMF was measured with a vibrating viscometer (AND SV-10) at 25°C and was calculated as the average of five tests at a concentration of 4 wt % (mol/v). The contact angle of a water drop (2 μL) on the polymer surface was measured with the sessile drop method with a contact shape analyzer (Krüss DA 100) for 25 min.

Thermal Analysis

Differential scanning calorimetry (DSC; TA Instruments DSC-Q20, New Castle, DE) was used to obtain calorimetry data from both the heating and cooling scans, which were performed at a rate of 10°C/min between −50 and 250°C. After melting at 250°C for 5 min and cooling quickly to −50°C, a 5-mg sample was heated to 250°C at 10°C/min and monitored for phase transitions. The soft-segment melting temperature (T_m) and

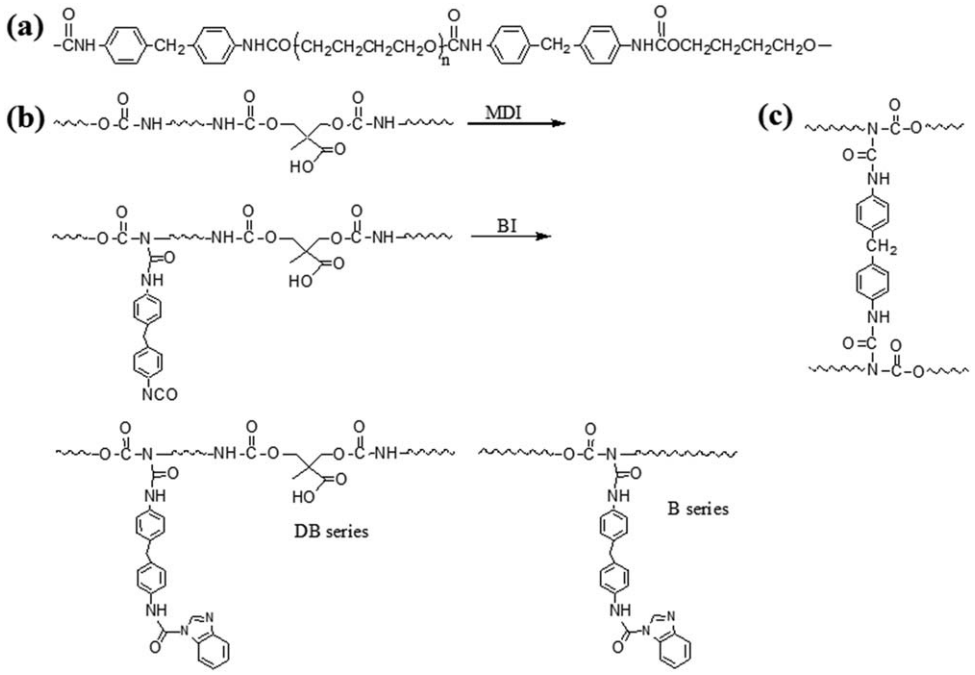

Scheme 1. (a) Structure of the unfunctionalized PU, (b) BI grafting onto PU with MDI for the DB and B series, and (c) possible crosslinking between PU chains.

enthalpy change during melting (ΔH_m) were determined with the Platinum software included with the DSC instrument. Thermogravimetric analysis (TGA; Seiko TG/DTA 200, Chiba, Japan) was used to monitor the thermal decomposition behavior of the samples as they were heated from 22 to 998°C at 10°C/min under a 50 mL/min nitrogen purge. Dynamic mechanical analysis (DMA) was used to collect the phase-transition data at low temperatures. Specifically, DMA (Trition TTDMA, Lincolnshire, United Kingdom) was used to measure the storage modulus (E') and loss modulus (E'') in the tension mode between −150 and 100°C at 10 Hz.

Tensile and Shape-Memory Tests

The tensile mechanical properties were measured according to the ASTM D 638 standard at 25°C with 0.5 mm thick samples. The measurements were collected on a universal testing machine (LR10K, West Sussex, Lloyd Materials Testing, United Kingdom) with a 20-mm gauge length, 20 mm/min crosshead speed, and 0.5-kN load cell. A total of seven specimens were tested for each group; the average tensile properties of five specimens, excluding the high and low values, are reported in this article. The same universal testing machine equipped with a temperature-controlled chamber was used for the cyclic shape-memory tests. A sample of length L_0 was drawn 100% to $2L_0$ in a temperature-controlled chamber at 45°C in 2 min, and the sample was kept at 45°C for 5 min. The upper grip was released after the specimen was cooled with liquid nitrogen to −25°C for 10 min, and then, the shrunken length (L_1) of the sample was measured. The percentage shape retention (%) was then calculated with eq. (1). In the chamber, the specimen was heated to 45°C for 10 min, and the length (L_2) was subsequently measured. The percentage shape recovery (%) was then calculated with eq. (2). The cyclic shape-memory test was repeated four times for each sample:

$$\text{Shape retention} = (L_1 - L_0) \times 100/L_0\,(\%) \quad (1)$$

$$\text{Shape recovery} = (2L_0 - L_2) \times 100/L_0\,(\%) \quad (2)$$

Antifungal Test

The antifungal tests were performed at Korea Textile Inspection and Testing Institute (Sungnam, Korea) according to ASTM G21-1996 with *Chaetomium globosum* (ATCC 6205). The test specimen (50 × 50 mm^2) was placed over the solidified nutrient-salt agar (3–6 mm thick) in a sterile Petri dish. We inoculated the whole agar surface, including the test specimen, by spraying the spore suspension from a sterilized atomizer with 110 kPa of air pressure. The inoculated test specimen was covered and incubated at 28°C and 91% humidity for 14 days. The antifungal effectiveness was visually evaluated on the basis of the fungal growth on a test specimen kept in a culture medium. The following ratings were used: 4 for heavy growth (over 60%), 3 for medium growth (30–60%), 2 for light growth (10–30%), 1 for traces of growth (<10%), and 0 for no growth.

RESULTS AND DISCUSSION

Synthesis and Structural Analysis of PU

PU can be functionalized by the covalent bonding of various functional groups to the chain. In particular, the carbamate bonding in PU can be used to graft functional groups onto the PU chains. The functionalization of the PU surface by grafting has been reported in the literature.[31–35] BI was selected as an antifungal agent because of its excellent effectiveness, and it was grafted onto PU via its nucleophilic imidazole group. MDI-3 was used as an activating agent to connect BI to PU to improve the binding and ensure its homogeneous distribution on the

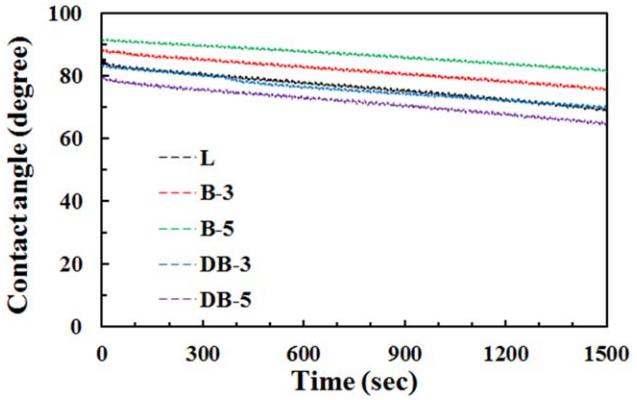

Figure 1. Water contact angle profiles for the B and DB series. [Color figure can be viewed in the online issue, which is available at wileyonlinelibrary.com.]

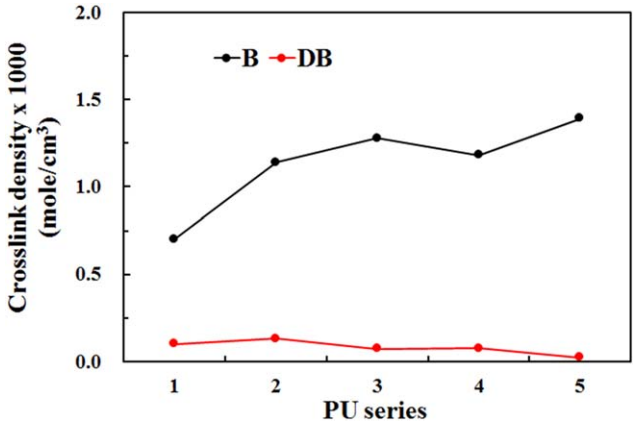

Figure 2. Crosslinking density profiles for the B and DB series. [Color figure can be viewed in the online issue, which is available at wileyonlinelibrary.com.]

PU. The BI grafting steps are shown in Scheme 1(b). As shown in Table I, the BI content increased gradually as the sample number increased for the B series, and the DMPA content increased, whereas the BI content was fixed in the DB series to ascertain the impact of the PU water compatibility on its properties. The water compatibilities of the PU surfaces were compared by the contact angles of the water drops on the PUs (Figure 1). The water contact angles of DB-3 and DB-5 were smaller than those of B-3 and B-5; this suggested that the DB series surface was more hydrophilic than that of the B series because of the carboxyl groups of DMPA. However, the decrease rate of the water contact angle was similar for both the B and DB series. Interestingly, the contact angle of DB-3 was close to that of the linear control polyurethane (L). Therefore, the contact angle results demonstrated that the carboxyl groups of the DB series increased the water compatibility of the PU surface. MDI-3 might also have acted as a crosslinker between the PU chains, as shown in Scheme 1(c), improving the mechanical strength of the grafted PU relative to that of the unfunctionalized PU. The crosslinking density was determined by PU swelling in toluene because it was inversely related to the degree of crosslinking. Specifically, the interaction parameter (χ) between toluene and PU was determined from the following expression:[36]

$$\chi = (\delta_1 - \delta_2)^2 V_1 / RT \quad (3)$$

where δ_1 and δ_2 are the solubility parameters of the solvent and polymer, respectively; V_1 is the solvent molar volume (106.3 cm^3/mol); R is the gas constant (8.31 $MPa \cdot cm^3 K^{-1} \cdot mol^{-1}$); and T is the absolute temperature (298 K).

δ_1 and δ_2 were 18.2 and 20.5 $MPa^{1/2}$, respectively.[37,38] The degree of crosslinking was calculated with the Flory–Rehner equation:

$$-\left[\ln(1-v_2) + v_2 + \chi v_2^2\right] = V_1 n \left[v_2^{1/3} - 1/2v_2\right] \quad (4)$$

where v_2 is the volume fraction of the polymer in the swollen mass and n is the crosslinking density.

The crosslinking density of the B series slowly increased with increasing BI content. However, the DB series had very low crosslinking densities, which decreased slightly with increasing DMPA content (Figure 2). The MDI crosslinking led to an increase in the crosslinking density of the B series,[39] and the DMPA in the DB series was responsible for the low crosslinking density because the DMPA carboxyl group might have prevented the close contact between the PU chains required for crosslinking. The small degree of crosslinking in the B series and the absence of crosslinking in the DB series impacted their observed tensile mechanical properties; this resulted in significantly different behaviors, as discussed in the following section.

The viscosities of the B and DB series in DMF were measured to determine the effects of the grafted BI and DMPA on the

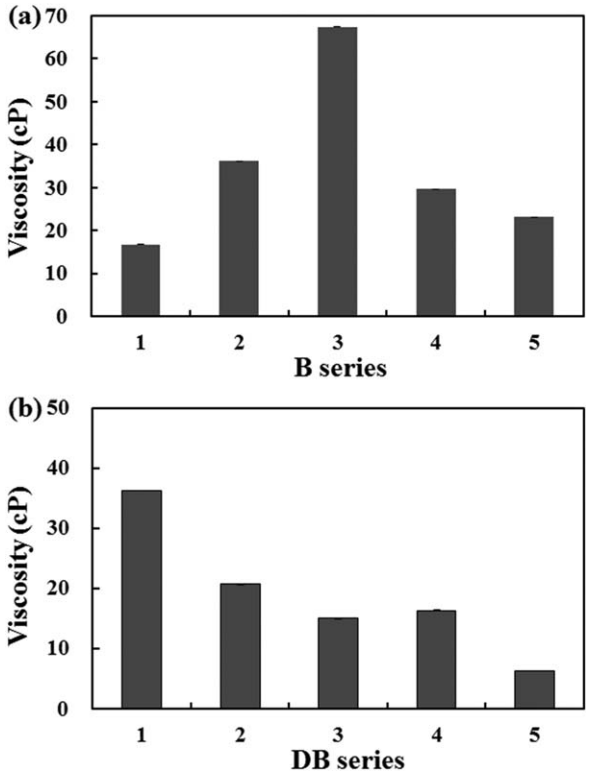

Figure 3. Viscosity profiles for the (a) B and (b) DB series.

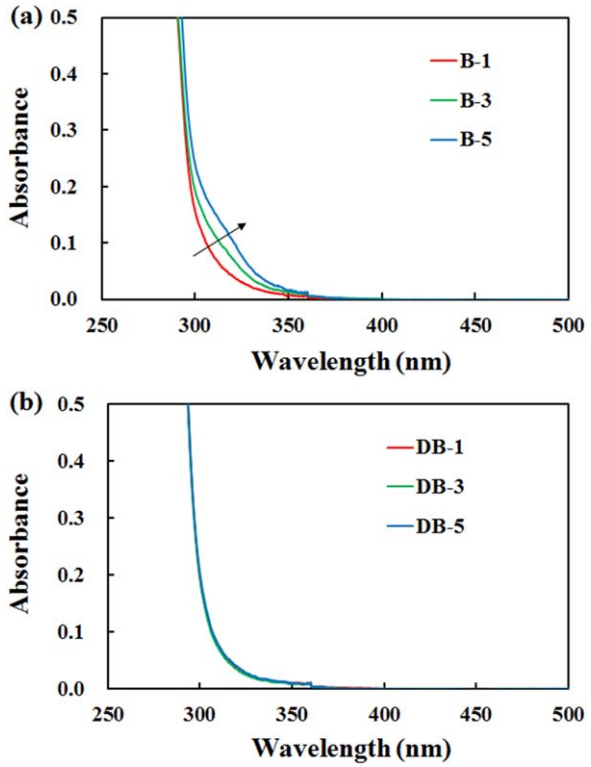

Figure 4. UV–vis spectra of the (a) B and (b) DB series. [Color figure can be viewed in the online issue, which is available at wileyonlinelibrary.com.]

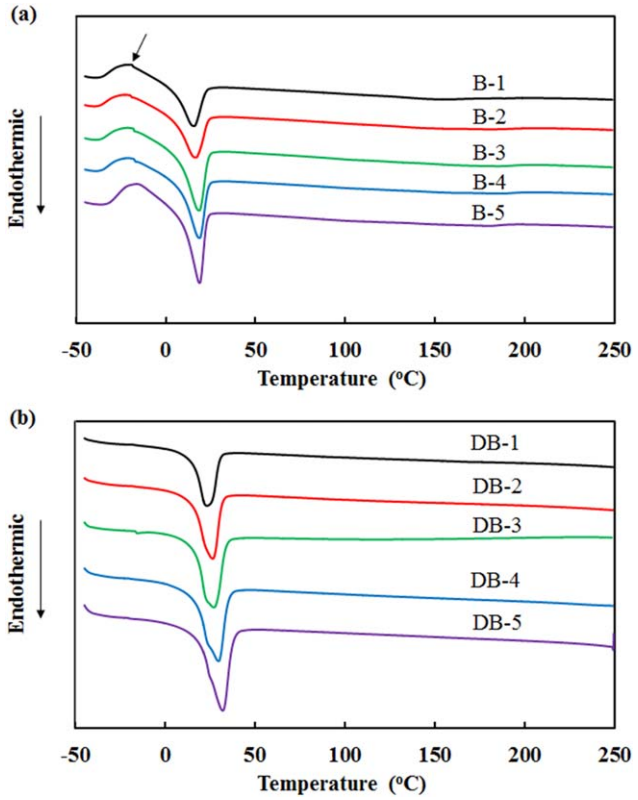

Figure 6. DSC thermograms of the (a) B and (b) DB series. [Color figure can be viewed in the online issue, which is available at wileyonlinelibrary.com.]

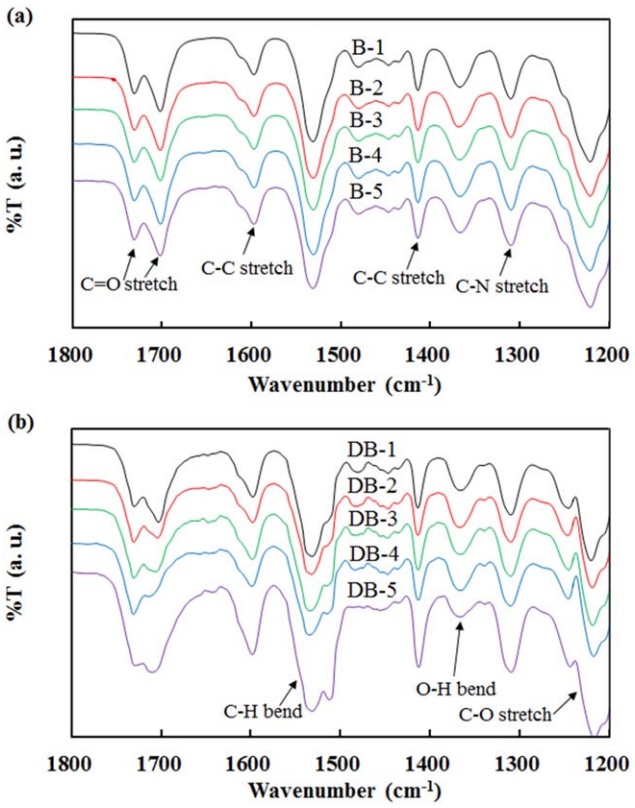

Figure 5. IR spectra of the (a) B and (b) DB series. [Color figure can be viewed in the online issue, which is available at wileyonlinelibrary.com.]

solution viscosity because they might have affected the molecular interactions between the PU chains. The viscosity results exhibited similar trends to the crosslinking density results: the B series viscosities initially increased as the BI content increased, and the DB series viscosities decreased with increasing DMPA content (Figure 3). The decrease in the B series viscosity observed at high BI contents was due to the repulsive interaction between the grafted BIs and the reduced drag between the PU chains. Therefore, the viscosity results demonstrated that DMPA disrupted the molecular interactions in the DB series, and the light crosslinking in the B series resulted in an increased viscosity. The UV–vis spectra were measured to analyze the BI groups grafted onto the PU. The BI peak at approximately 320 nm increased with increasing BI content in the B series [Figure 4(a)]. However, the UV–vis spectra of the DB series were similar because the BI content was the same for all of the DB samples [Figure 4(b)]. The UV–vis spectra demonstrated that the amount of BI grafted onto the PU was determined by the amount of BI used in the synthesis (see Table I).

IR and Thermal Analysis

The IR spectra exhibited peaks assigned to C—H bending at 1527 cm^{-1}, aromatic C—C ring stretching at 1592 and 1411 cm^{-1}, O—H bending at 1362 cm^{-1}, C—N stretching at 1305 cm^{-1}, and C—O stretching at 1215 cm^{-1}. These peaks were observed for both the B and DB series (Figure 5). The C═O stretching peaks at approximately 1700 and 1730 cm^{-1} were used to analyze the intermolecular interactions, such as hydrogen bonding and dipole–dipole interactions, between the

Table II. Comparison of the Soft-Segment Thermal Properties of the PU Series

Sample code	T_m (°C)	ΔH_m (J/g)	T_g (°C)[a]
B-1	15.1	30.1	−67.1
B-2	16.0	31.2	−65.4
B-3	18.3	34.1	−64.0
B-4	18.5	35.5	−65.3
B-5	18.7	40.0	−64.1
DB-1	23.2	37.4	−60.2
DB-2	26.4	39.2	−58.1
DB-3	27.3	39.5	−53.6
DB-4	29.7	44.0	−45.9
DB-5	31.9	46.4	−42.9

[a] T_g was determined from the E'' data.

hard segments. The bonded carbonyl band (1700 cm^{-1}) appeared at a lower wave number than the free carbonyl group band (1730 cm^{-1}).[24] The relative intensities of the bonded and free carbonyl stretches indicated the degree of phase separation (DPS) that occurred when the molecular interactions between the hard segments changed. The DPS was calculated with the equation DPS = $A_{1700}/(A_{1730} + A_{1700})$, where A_{1700} and A_{1730} are the absorbances at 1700 and 1730 cm^{-1}, respectively. The DPS of the B series varied slightly from 56.5% for B-1 to 57.5% for B-3 and 56.0% for B-5. However, the DPS of the DB series varied drastically from 56.5% for DB-1 to 47.5% and 51.7% for DB-3 and DB-5, respectively. These results suggested that the molecular interactions were not affected by the BI content in the B series, but they were significantly influenced by the DMPA content in the DB series.

The soft-segment T_m's of the B and DB series were measured by DSC. The melting peak of the soft segment was observed between 15 and 32°C during the second heating scan (Figure 6). The T_m's and ΔH_m's of melting are listed in Table II. The T_m increased as the BI and DMPA contents increased in the B and DB series, respectively. For example, T_m increased from 15.1°C for B-1 to 18.7°C for B-5 and from 23.2°C for DB-1 to 31.9°C for DB-5. The ΔH_m values also increased significantly as the BI and DMPA contents increased in the B and DB series, respectively. Specifically, ΔH_m increased from 30.1 J/g for B-1 to 40.0 J/g for B-5 and from 37.4 J/g for DB-1 to 46.4 J/g for DB-5. The rigid BI structure and the crosslinking by MDI-3 restricted the movement of the B series PU; this resulted in an increase in ΔH_m as the BI content increased. Similarly, the DMPA carboxyl groups restricted the movement of the DB series PU, and ΔH_m thus increased as the DMPA content increased. The glass-transition temperature (T_g) of the soft segments was measured by DMA, which involved the monitoring of E' and E'' between −150 and 100°C (Figure 7). A rapid decrease in E' and the appearance of a E'' peak, which were indicative of the soft-segment glass transition, were observed at approximately −60°C. The T_g data given in Table II are based on E'' peaks. The T_g increased as the BI and DMPA contents increased: T_g increased from −67.1°C for B-1 to −64.0°C for B-3 and −64.1°C for B-5 and from −60.2°C for DB-1 to −53.6°C for DB-3 and −42.9°C for DB-5. The increase in T_g observed for the DB series was greater than that observed for the B series; this suggested that DMPA restricted the PU chain rotation in the DB series more than the grafted BI did in the B series. The DB crystallization peaks at approximately −15°C completely disappeared as the DMPA content increased, whereas the B crystallization peaks at approximately −23°C were not significantly affected by the BI content. The disappearance of crystallization peaks was also observed in the DSC plot (Figure 6), in which the crystallization

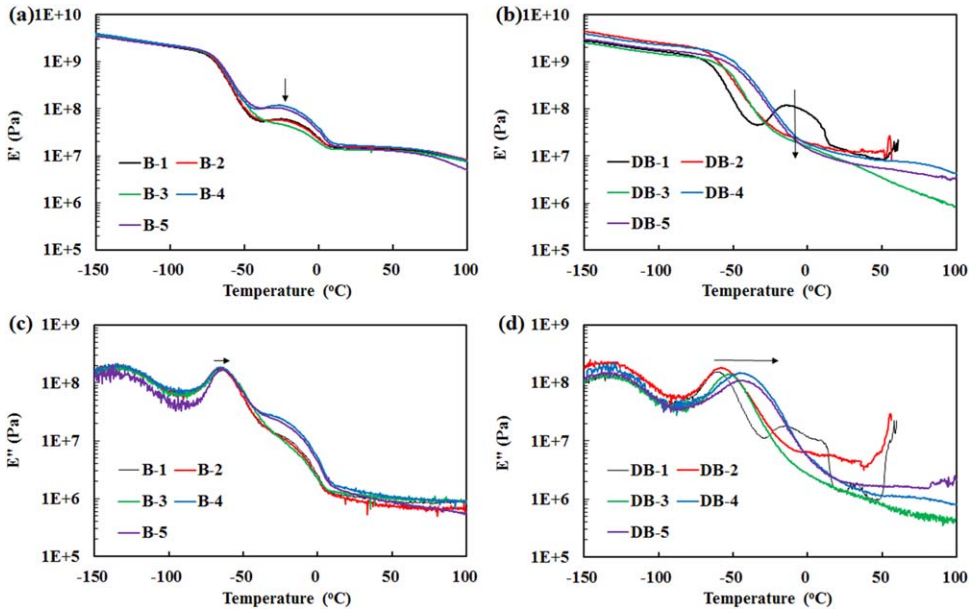

Figure 7. E' profiles for the (a) B and (b) DB series and E'' profiles for the (c) B and (d) DB series. [Color figure can be viewed in the online issue, which is available at wileyonlinelibrary.com.]

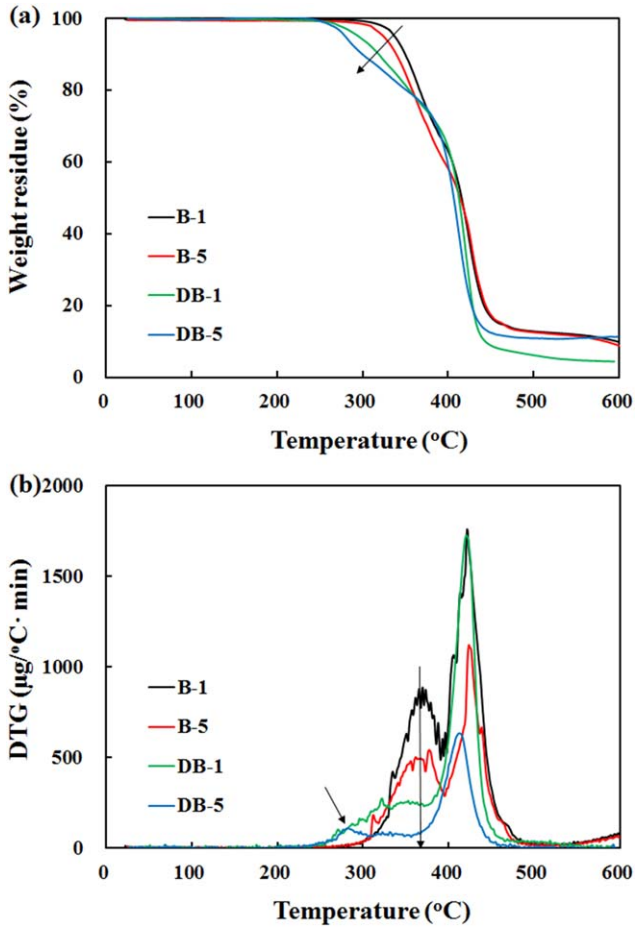

Figure 8. (a) TGA and (b) first-derivative profiles for the B and DB series. Differential thermogravimetric (DTG) curve is the rate of mass loss versus temperature. [Color figure can be viewed in the online issue, which is available at wileyonlinelibrary.com.]

peaks in the B series at approximately −18°C disappeared in the DB series. The crystallization peak results also demonstrated that DMPA had a larger effect on the PU chain alignment than the grafted BI did. The thermal decomposition of the B and DB series was analyzed by TGA (Figure 8). For the B series, two decomposition steps were observed. The first decomposition step at approximately 370°C corresponded to the decarboxylation of the PU carbamate bond, and the second decomposition step at approximately 420°C was due to the thermal decomposition of the remaining PU hydrocarbons. For the DB series, the decarboxylation was observed at a lower temperature (ca. 280°C) because of the decarboxylation of DMPA. The shift in the decarboxylation temperature was clearly observed in the derivatized TGA curves: in the DB series curves, the B series decomposition peak at 370°C decreased considerably, and a decomposition peak was observed at a lower temperature. Therefore, the differences in the B and DB series in TGA thermograms indicated the presence of DMPA in the DB series. The combined thermal analysis results suggest that the T_g, T_m, and ΔH_m values of the B and DB series were affected by the grafted BI and DMPA.

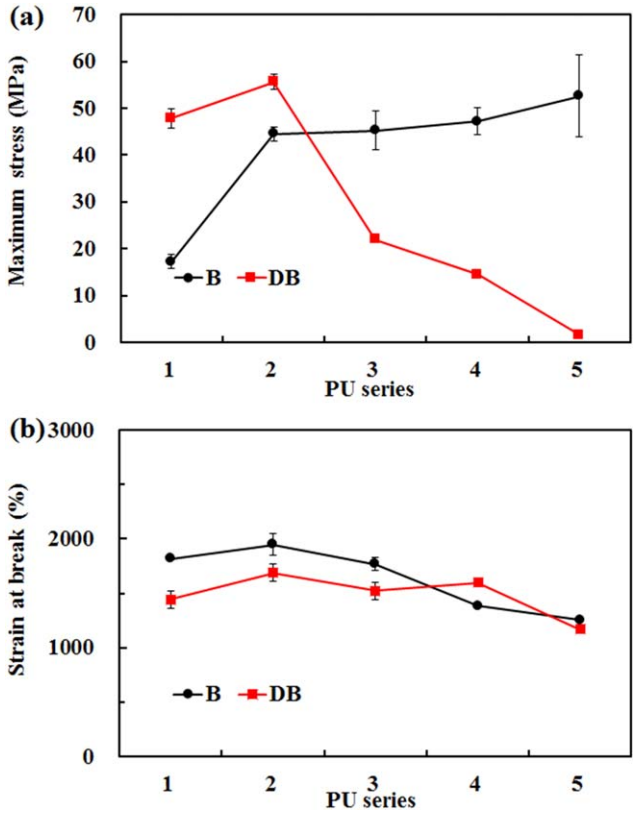

Figure 9. (a) Maximum stress and (b) breaking strain profiles for the B and DB series. [Color figure can be viewed in the online issue, which is available at wileyonlinelibrary.com.]

Tensile and Shape-Memory Properties

The maximum tensile stress of the B series was significantly greater than that of L (B-1). However, the maximum tensile stress of the DB series decreased considerably with increasing DMPA content [Figure 9(a)]. For example, the maximum tensile stress increased from 17.2 MPa for B-1 to 45.2 MPa for B-3 and 52.6 MPa for B-5, whereas it decreased from 47.8 MPa for DB-1 to 22.0 MPa for DB-3 and 1.5 MPa for DB-5. The

Table III. Shape-Memory Properties

	Recovery (%)		Retention (%)	
Sample code	First[a]	Fourth[a]	First	Fourth
B-1	93	97	96	96
B-2	90	86	95	96
B-3	86	84	95	96
B-4	91	93	96	87
B-5	89	84	96	100
DB-1	92	88	96	98
DB-2	96	94	90	85
DB-3	86	86	98	98
DB-4	93	91	96	97
DB-5	87	85	99	99

[a] Shape-memory results for the first and fourth test cycles.

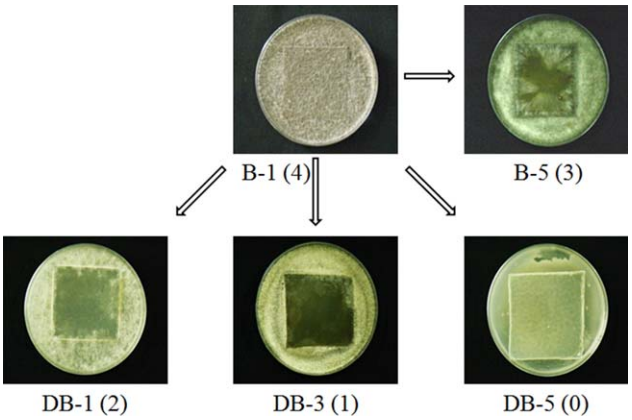

Figure 10. Antifungal tests against *C. globosum* (ATCC 6205): the number in parentheses indicates the rating [heavy growth (4), medium growth (3), light growth (2), traces of growth (1), and none (0)]. [Color figure can be viewed in the online issue, which is available at wileyonlinelibrary.com.]

increase in the maximum stress for the B series was due to the crosslinking shown in Scheme 1(c), and the sharp decrease in the maximum stress for the DB series originated from the repulsion between the DMPA carboxyl groups and the reduced crosslinking observed for this series. The breaking strain decreased slightly with increasing BI and DMPA contents in the B and DB series, respectively: it decreased from 1818% for B-1 to 1767% for B-3 and 1255% for B-5 and from 1445% for DB-1 to 1524% for DB-3 and 1167% for DB-5 [Figure 9(b)]. Thus, the crosslinking in the B series and DMPA in the DB series did not reduce the tensile strain considerably. The tensile test results revealed that the DMPA content had a significant impact on the PU tensile strength.

Shape-memory tests were conducted repeatedly for the B and DB series between −25 and 45°C. The soft-segment T_m was used as the reference temperature for the shape-memory tests because the T_m was close to room temperature, and this was useful for practical applications.[40,41] The shape recovery of the B series was slightly better than that of the DB series. The BI and DMPA contents in the B and DB series did not significantly affect the shape-recovery results. The shape-recovery results for both series were reproducible, as demonstrated by repetition of the test cycle four times (Table III). For example, the shape recoveries of B-1, B-5, DB-1, and DB-5 varied from 92, 93, 88, and 91%, respectively, for the first test cycle to 96, 92, 84, and 88%, respectively, for the fourth test cycle. Therefore, the B and DB series did not lose their ability to recover their shape or their recovery efficiency after repeated stretching and shrinking cycles. The shape retention was similar for the B and DB series and was also not affected by the BI and DMPA contents in the B and DB series, respectively. The shape retention decreased slightly as the number of test cycles increased for both series. For example, the shape retentions of B-1, B-5, DB-1, and DB-5 varied from 99, 92, 96, and 90%, respectively, for the first test cycle to 98, 87, 96, and 92%, respectively, for the fourth test cycle. Although the DMPA in the DB series significantly reduced the tensile strength, the shape-memory properties were unaffected by the DMPA content.

Antifungal Activity Testing

The selected B and DB samples were tested for antifungal activity against *C. globosum,* and their effectiveness is compared in Figure 10. The antifungal effectiveness was evaluated on the basis of the fungal growth after the incubation period and rated as follows: 4 for heavy growth (over 60%), 3 for medium growth (30–60%), 2 for light growth (10–30%), 1 for traces of growth (<10%), and 0 for no growth. B-1, which did not contain BI, did not exhibit any antifungal activity, and its antifungal effectiveness was assigned a value of 4. B-5, which had the highest BI content, did not satisfactorily suppress the fungal growth and was given a rating of 3. DB-1 and DB-3, which had the same BI content and different DMPA contents, were given ratings of 2 and 1, respectively; this means that DB-3 exhibited a higher antifungal activity than DB-1. Finally, DB-5 completely suppressed the fungal growth on the sample and was assigned a rating of 0. As a control experiment, DB-5 without BI and MDI-3 was separately prepared by the same method and tested for the antifungal activity. However, it was rejected for the antifungal test from the test institute because of its stickiness and fragile structure. The antifungal test results that the DMPA content played a vital role in controlling the fungal growth in contrast to the BI content; this suggested that PU must be water-compatible for the BI grafted onto PU to exhibit full antifungal activity. The higher water compatibility of DB-5, compared to those of L, B-3, B-5, and DB-3, was already confirmed in the water contact angle results, as shown in Figure 1. Therefore, the incorporation of both BI and DMPA into PU resulted in a high antifungal activity.

CONCLUSIONS

Two PU series, one with grafted BI (B series) and the second with grafted BI and inserted DMPA (DB series), were prepared to examine their antifungal activities. BI was used as the antifungal agent, and DMPA was included to improve the PU water compatibility, which was demonstrated in the water contact angle results of the PU surfaces. The crosslinking density increased with increasing BI content in the B series and decreased with increasing DMPA content in the DB series. The grafted BI and DMPA contents affected the T_g, T_m, and ΔH_m values of both series. The tensile strength of the B series increased with increasing BI content, whereas that of the DB series decreased with increasing DMPA content. For both series, the shape recovery and retention remained high and were reproducible, as demonstrated by the cyclic test results, even as the BI and DMPA contents increased. The DB series exhibited a higher antifungal activity than the B series because of its enhanced water compatibility. Therefore, the BI-grafted PU needed a water-compatible structure to exhibit full antifungal activity.

ACKNOWLEDGMENTS

This work was supported by the 2014 Postmaster Research Program of Inje University. This study was supported by the R&D Center for Valuable Recycling (Global-Top Environmental Technology Development Program) funded by the Ministry of Environment (contract grant number 2014001190001).

REFERENCES

1. El-Refaie, K.; Worley, S. D.; Broughton, R. *BioMacromolecules* **2007**, *8*, 1359.
2. Rogalskyy, S.; Bardeau, J. F.; Tarasyuk, O.; Fatyeyeva, K. *Polym. Int.* **2012**, *61*, 686.
3. Liu, R.; Chen, X.; Hayouka, Z.; Chakraborty, S.; Falk, S. P.; Weisblum, B.; Masters, K. S.; Gellman, S. H. *J. Am. Chem. Soc.* **2013**, *135*, 5270.
4. Vlad, S.; Tanase, C.; Macocinschi, D.; Ciobanu, C.; Balaes, T.; Filip, D.; Gostin, I. N.; Gradinaru, L. M. *Dig. J. Nanomater. Bios.* **2012**, *7*, 51.
5. Meng, N.; Zhou, N. L.; Zhang, S. Q.; Shen, J. *Appl. Clay Sci.* **2009**, *46*, 136.
6. Paladini, F.; Cooper, I. R.; Pollini, M. *J. Appl. Microbiol.* **2014**, *116*, 710.
7. Napoli, M.; Saturnino, C.; Cianciulli, E. I.; Varcamonti, M.; Zanfardino, A.; Tommonaro, G.; Longo, P. *J. Organomet. Chem.* **2013**, *725*, 46.
8. Ruan, B.; Tian, Y.; Zhou, H.; Wu, J.; Liu, Z.; Zhu, C.; Yang, J.; Zhu, H. *J. Organomet. Chem.* **2009**, *694*, 2883.
9. Patel, R. V.; Patel, P. K.; Kumari, P.; Rajani, D. P.; Chikhalia, K. H. *Eur. J. Med. Chem.* **2012**, *53*, 41.
10. Kücükbay, H.; Durmaz, R.; Orhan, E.; Günal, S. *Il Farm.* **2003**, *58*, 431.
11. Ansari, K. F.; Lal, C. *Eur. J. Med. Chem.* **2009**, *44*, 4028.
12. Kalinowska-Lis, U.; Felczak, A.; Checinska, L.; Lisowska, K.; Ochocki, J. *J. Organomet. Chem.* **2014**, *749*, 394.
13. Sheehan, D. J.; Hitchcock, C. A.; Sibley, C. M. *Clin. Microbiol. Rev.* **1999**, *12*, 40.
14. Song, S.; Kim, J.; Shim, J. Y.; Kim, G.; Lee, B. H.; Jin, Y.; Park, S. H.; Kim, I.; Lee, K.; Suh, H. *Synth. Met.* **2012**, *162*, 988.
15. Song, S.; Park, S. H.; Jin, Y.; Kim, I.; Lee, K.; Suh, H. *Polymer* **2012**, *51*, 5385.
16. Linlin, M.; Mishra, A. K.; Kim, N. H.; Lee, J. H. *J. Membr. Sci.* **2012**, *411*, 91.
17. Tan, N.; Chen, Y.; Xiao, G.; Yan, D. *J. Membr. Sci.* **2012**, *356*, 70.
18. Kim, S. K.; Kim, K. H.; Park, J. O.; Kim, K.; Ko, T.; Choi, S. W.; Pak, C.; Chang, H.; Lee, J. C. *J. Power Sources* **2013**, *226*, 346.
19. Choi, H.; Chung, I. S.; Hong, K.; Park, C. E.; Kim, S. Y. *Polymer* **2008**, *49*, 2644.
20. Maurya, M. R.; Sikarwar, S.; Joseph, T.; Manikandan, P.; Halligudi, S. B. *React. Funct. Polym.* **2005**, *63*, 71.
21. Takahashi, T.; Hayashi, N.; Hayashi, S. *J. Appl. Polym. Sci.* **1996**, *60*, 1061.
22. Chen, L. W.; Lin, J. R. *J. Appl. Polym. Sci.* **1998**, *69*, 1575.
23. Wang, W.; Ping, P.; Chen, X.; Jing, X. *Eur. Polym. J.* **2006**, *42*, 1240.
24. Chung, Y. C.; Park, H. S.; Choi, J. W.; Chun, B. C. *High Perform. Polym.* **2012**, *24*, 200.
25. Chung, Y. C.; Park, J. S.; Shin, C. H.; Choi, J. W.; Chun, B. C. *Macromol. Res.* **2012**, *20*, 66.
26. Chung, Y. C.; Choi, J. W.; Choi, M. W.; Chun, B. C. *J. Thermoplast. Compos.* **2012**, *25*, 283.
27. Chung, Y. C.; Jung, I. H.; Choi, J. W.; Chun, B. C. *Polym. Bull.* **2014**, *71*, 1153.
28. Chung, Y. C.; Choi, J. W.; Lee, S. H.; Chun, B. C. *Bull. Kor. Chem. Soc.* **2011**, *32*, 2988.
29. Tischer, M.; Pradel, G.; Ohlsen, K.; Holzgrabe, U. *ChemMedChem* **2012**, *7*, 22.
30. Kenawy, E.-R.; Abdel-Hay, F. I.; El-Magd, A. A.; Mahmoud, Y. *React. Funct. Polym.* **2006**, *66*, 419.
31. Freij-Larsson, C.; Wesslen, B. *J. Appl. Polym. Sci.* **1993**, *50*, 345.
32. Archambault, J. G.; John, L. *Colloid Surf. B* **2004**, *39*, 9.
33. Tan, K.; Obendorf, S. K. *J. Membr. Sci.* **2006**, *274*, 150.
34. Alves, P.; Coelho, J. F. J.; Haack, J.; Rota, A.; Bruinink, A.; Gil, M. H. *Eur. Polym. J.* **2009**, *45*, 1412.
35. Huang, J.; Xu, W. *Appl. Surf. Sci.* **2010**, *256*, 3921.
36. Petrovic, Z. S.; Javni, I.; Divjakovic, V. J. *J. Polym. Sci. Part B: Polym. Phys.* **1998**, *36*, 221.
37. Sekkar, V.; Gopalakrishnan, S.; Devi, K. A. *Eur. Polym. J.* **2003**, *39*, 1281.
38. Sekkar, V.; Rama Rao, M.; Krishinamurthy, V. N.; Jane, S. R. *J. Appl. Polym. Sci.* **1996**, *62*, 2317.
39. Chung, Y. C.; Choi, J. W.; Chung, H. M.; Chun, B. C. *Bull. Kor. Chem. Soc.* **2012**, *33*, 692.
40. Hu, J.; Yang, Z.; Yeung, L.; Ji, F.; Liu, Y. *Polym. Int.* **2005**, *54*, 54.
41. Zhuohonga, Y.; Jinliana, H.; Yeqiua, L.; Lapyana, Y. *Mater. Chem. Phys.* **2006**, *98*, 368.